

Asymptotic power-law tails of massive scalar fields in a Reissner-Nordström background

Hiroko Koyama* and Akira Tomimatsu†

Department of Physics, Nagoya University, Nagoya 464-8602, Japan

(Received 5 December 2000; published 23 February 2001)

We investigate the dominant late-time tail behavior of massive scalar fields in a nearly extreme Reissner-Nordström background. It is shown that the oscillatory tail of the scalar fields has the decay rate of $t^{-5/6}$ at asymptotically late times. The physical mechanism by which the asymptotic $t^{-5/6}$ tail is generated and the relation between the field mass and the time scale when the tail begins to dominate are discussed in terms of resonance backscattering due to space-time curvature.

DOI: 10.1103/PhysRevD.63.064032

PACS number(s): 04.20.Ex, 04.70.Bw

I. INTRODUCTION

Various interactions of black holes with scalar fields have been extensively studied for a long time. Though previous works have been mainly concerned with the evolution of a massless scalar field, the analysis of massive ones will be also physically important. For example, in higher-dimensional theories, the Fourier modes of a massless scalar field behave like massive fields known as Kaluza-Klein modes, and the recent development of the Kaluza-Klein idea (e.g., the Randall-Sundrum model [1] in string theory) strongly motivates us to understand the evolutionary features due to the field mass in detail.

Massive scalar fields in black-hole space times can cause interesting phenomena which are qualitatively different from the massless case. A remarkable example is the vacuum polarization $\langle \phi^2 \rangle$ of a quantum massive scalar field ϕ , which is in thermal equilibrium with a nearly extreme Reissner-Nordström black hole [2]. Because the black-hole temperature is very low, the mass-induced excitation of $\langle \phi^2 \rangle$ results in the resonant amplification at $mM \approx O(1)$ for the field mass m and the black-hole mass M .

Such a resonance behavior due to the mass of a field interacting with a black hole may appear in various processes as a basic feature of black-hole geometry. For a step to support this conjecture, in this paper, we turn our attention to the problem of time evolution of classical fields.

The evolution of a massive scalar field in Schwarzschild background was analyzed by Starobinskii and Novikov, using the complex plane approach [3], and they found that because of the mass term, there are poles in the complex plane closer to the real axis than in the massless case, which leads to inverse power-law behavior with smaller indices than the massless case. Recently, it was pointed out that the late-time tails of massive scalar fields in Reissner-Nordström space time are quite different from massless fields in the existence of the intermediate late-time tails [4]. If the field mass m is small, namely $mM \ll 1$, the oscillatory inverse power-law behavior

$$\psi \sim t^{-l-(3/2)} \sin(mt) \quad (1)$$

dominates as the intermediate late-time tails. Note that massless fields decay more rapidly without any oscillation, as was studied by Price [6]. The analytical approximation (1) was derived from the flat-space-time approximation, where the effects of space-time curvature are neglected. Though the behavior (1) was numerically verified at intermediate late times, Hod and Piran [4] also suggested that another wave pattern dominates at very late times, namely the intermediate tails (1) are not final asymptotic behaviors, and they mentioned that “fields decay at late times slower than any power law.” Though similar numerical results in the Schwarzschild case were reported by Burko [5], the evolution of massive scalar fields at asymptotic late times has been claimed to be inverse power-law behavior.

The purpose of this paper is to clarify what kind of mass-induced behaviors dominates in the asymptotic late-time tails as a result of interaction of massive scalar fields with a black hole. In Sec. II we introduce the black-hole Green’s function using the spectral decomposition method [7]. (Another method to treat late-time tails which is called “late time expansions” was also proposed recently [8].) In Sec. III we consider a nearly extreme Reissner-Nordström background, motivated by the fact that the resonance phenomena in the vacuum polarization of quantum scalar fields become clear. Then, based on the procedure of asymptotic matching, we construct approximate solutions in the nearly extreme limit. In Sec. IV we study the intermediate tail which appears in the case of a small mass field, confirming our result in comparison with Eq. (1). In Sec. V we derive the asymptotic late-time tail which is the main result in this paper. Section VI is devoted to a summary and discussion.

II. GREEN’S-FUNCTION ANALYSIS

A. Massive scalar fields in Reissner-Nordström geometry

We consider time evolution of a massive scalar field in the Reissner-Nordström background with mass M and charge Q . The metric is

$$ds^2 = - \left(1 - \frac{2M}{r} + \frac{Q^2}{r^2} \right) dt^2 + \left(1 - \frac{2M}{r} + \frac{Q^2}{r^2} \right)^{-1} dr^2 + r^2 d\Omega^2, \quad (2)$$

*Email address: hiroko@allegro.phys.nagoya-u.ac.jp

†Email address: atomi@allegro.phys.nagoya-u.ac.jp

and the scalar field ϕ with mass m satisfies the wave equation

$$(\square - m^2)\phi = 0. \quad (3)$$

Resolving the field into spherical harmonics

$$\phi = \sum_{l,m} \frac{\psi_l(t,r)}{r} Y_l^m(\theta, \varphi), \quad (4)$$

we obtain a wave equation for each multiple moment,

$$\psi_{,tt} - \psi_{,r_* r_*} + V\psi = 0, \quad (5)$$

where r_* is the tortoise coordinate defined by

$$dr_* = \frac{dr}{1 - \frac{2M}{r} + \frac{Q^2}{r^2}}, \quad (6)$$

and the potential V is

$$V = \left(1 - \frac{2M}{r} + \frac{Q^2}{r^2}\right) \left[\frac{l(l+1)}{r^2} + \frac{2M}{r^3} - \frac{2Q^2}{r^4}\right]. \quad (7)$$

B. The black-hole Green's function

The time evolution of ψ is given by

$$\psi(r_*, t) = \int [G(r_*, r'_*; t) \psi_t(r', 0) + G_t(r_*, r'_*; t) \psi(r'_*, 0)] dr'_* \quad (8)$$

for $t > 0$, where $G(r_*, r'_*; t)$ is the (retarded) Green's function satisfying

$$\left[\frac{\partial^2}{\partial t^2} - \frac{\partial^2}{\partial r_*^2} + V\right] G(r_*, r'_*; t) = \delta(t) \delta(r_* - r'_*) \quad (9)$$

with the initial condition $G(r_*, r'_*; t) = 0$ for $t \leq 0$. We calculate the Green's function through the Fourier transform

$$G(r_*, r'_*; t) = -\frac{1}{2\pi} \int_{-\infty+ic}^{\infty+ic} \tilde{G}(r_*, r'_*; \omega) e^{-i\omega t} d\omega, \quad (10)$$

where c is some positive constant. The usual procedure is to close the contour of integration into the lower half of the complex frequency plane shown in Fig. 1. Then, the late-time tail behaviors which are our main concern should be given by the integral along the branch cut placed along the interval $-m \leq \omega \leq m$.

The Fourier component $\tilde{G}(r_*, r'_*; \omega)$ in the range $-m \leq \omega \leq m$ can be expressed in terms of two linearly independent solutions $\tilde{\psi}_1$ and $\tilde{\psi}_2$ for the homogeneous equation

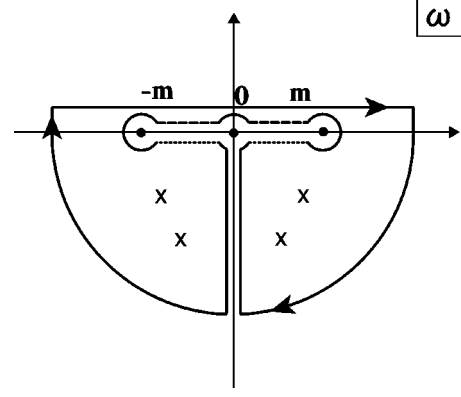


FIG. 1. Integration contours in the complex frequency plane. The original integration contour for the Green's function lies above the real frequency axis. We choose the value of ϖ on the dashed line to be $\varpi = |\varpi|$ and that on the dotted lines to be $\varpi = e^{\pm i\pi} |\varpi|$. The poles in $\tilde{G}(r_*, r'_*; \omega)$ are also shown, which give the quasinormal modes.

$$\left(\frac{d^2}{dr_*^2} + \omega^2 - V\right) \tilde{\psi}_i = 0, \quad i=1,2. \quad (11)$$

The boundary condition for the basic solution $\tilde{\psi}_1$ is to describe purely ingoing waves crossing the event horizon, i.e.,

$$\tilde{\psi}_1 \simeq e^{-i\omega r_*}, \quad (12)$$

as $r_* \rightarrow -\infty$, while $\tilde{\psi}_2$ is required to damp exponentially at spatial infinity, i.e.,

$$\tilde{\psi}_2 \simeq e^{-\varpi r_*}, \quad (13)$$

as $r_* \rightarrow \infty$, where $\varpi \equiv \sqrt{m^2 - \omega^2}$. Because the complex conjugate $\tilde{\psi}_1^*$ is also a solution for Eq. (11), $\tilde{\psi}_2$ can be written by the linear superposition

$$\tilde{\psi}_2 = \alpha \tilde{\psi}_1 + \beta \tilde{\psi}_1^*, \quad (14)$$

and the Wronskian is estimated to be

$$W(\omega) = \tilde{\psi}_1 \tilde{\psi}_{2,r_*} - \tilde{\psi}_{1,r_*} \tilde{\psi}_2 = 2i\omega\beta. \quad (15)$$

Using these two solutions, the Green's function can be written by

$$\tilde{G}(r_*, r'_*; \omega) = -\frac{1}{2i\omega\beta} \begin{cases} \tilde{\psi}_1(r'_*, \omega) \tilde{\psi}_2(r_*, \omega), & r' > r \\ \tilde{\psi}_1(r_*, \omega) \tilde{\psi}_2(r'_*, \omega), & r' < r. \end{cases} \quad (16)$$

The contribution G^C from the branch cut to the Green's function is reduced to

$$\begin{aligned}
G^C(r_*, r'_*; t) &= -\frac{1}{4\pi i} \int_{\text{cut}} \frac{1}{\omega} \frac{\alpha}{\beta} \tilde{\psi}_1(r'_*, \omega) \tilde{\psi}_1(r_*, \omega) e^{-i\omega t} d\omega. \\
&= -m^2 r_+^2 \left\{ (z-1)\kappa r_+ + 1 \right\}^2 \\
&\quad - \frac{\kappa r_+^2 \{2\kappa r_+^2 + z(r_+ + r_-)\}}{r_+^2 \{(z-1)\kappa r_+ + 1\}^2} \tilde{\psi} = 0. \tag{19}
\end{aligned}$$

Then the main task to evaluate G^C is to derive the coefficients α and β .

For the nearly extreme case such that

III. NEARLY EXTREME LIMIT

$$\kappa M \ll 1, \tag{20}$$

It is difficult in general to obtain the coefficients α and β , since exact solutions for the wave equation (11) cannot be expressed by any elementary function or any transcendental function already known. Fortunately, in nearly extreme Reissner-Nordström geometry, the procedure of asymptotic matching turn out to be very useful. Let us change the variable r to z defined as

$$\frac{z-1}{2} = \frac{r-r_+}{2\kappa r_+^2}, \tag{18}$$

where r_+ and r_- are the outer and inner horizon radii, respectively, and κ is the surface gravity defined as $\kappa \equiv (r_+ - r_-)/2r_+^2$. Then we can rewrite the wave equation (11) into

we can derive the approximate solutions valid in the region $z \gg 1$ or $z \ll 1/\kappa M$.

A. Solutions for $z \ll 1/\kappa M$

Expanding the wave equation (19) as a power series in $\kappa M z$ and truncating terms of order $\kappa M z$ and higher, we obtain

$$\begin{aligned}
(z^2-1) \frac{d^2 \tilde{\psi}}{dz^2} + 2z \frac{d\tilde{\psi}}{dz} + \left[\frac{1}{z^2-1} \frac{\omega^2}{\kappa^2} \right. \\
+ \frac{1}{z+1} \left(\frac{4\omega^2 M}{\kappa} - 12\omega^2 M^2 \right) \\
\left. + \{6\omega^2 M^2 - l(l+1) - m^2 M^2\} \right] \tilde{\psi} = 0. \tag{21}
\end{aligned}$$

$$\begin{aligned}
(z^2-1) \frac{d^2 \tilde{\psi}}{dz^2} + \frac{\{2\kappa r_+^2 + z(r_+ + r_-)\}}{r_+ \{(z-1)\kappa r_+ + 1\}} \frac{d\tilde{\psi}}{dz} \\
+ \left[\frac{\omega^2 \{(z-1)\kappa r_+ + 1\}^4}{\kappa^2 (z^2-1)} - l(l+1) \right] \tilde{\psi} = 0.
\end{aligned}$$

Then the solution $\tilde{\psi}_1$ satisfying the boundary condition (12) can be written using the hypergeometric function F ,

$$\tilde{\psi}_1(\omega, r_*) = \xi^{(i\omega/\kappa) - 2i\omega M + (1/2) + \mu} (\xi - 1)^{-(i\omega/2\kappa)} F\left(-\frac{i\omega}{\kappa} + 2i\omega M - \mu + \frac{1}{2}, -2i\omega M - \mu + \frac{1}{2}, -\frac{i\omega}{\kappa} + 1; \frac{\xi - 1}{\xi}\right) \tag{22}$$

$$\begin{aligned}
&= \xi^{(i\omega/\kappa) - 2i\omega M - \mu + (1/2)} (\xi - 1)^{-(i\omega/2\kappa)} \frac{\Gamma\left(\frac{i\omega}{\kappa} + 1\right) \Gamma(-2\mu)}{\Gamma\left(\frac{i\omega}{\kappa} - 2i\omega M - \mu + \frac{1}{2}\right) \Gamma\left(2i\omega M - \mu + \frac{1}{2}\right)} \\
&\quad \times F\left(2i\omega M + \mu + \frac{1}{2}, \frac{i\omega}{\kappa} - 2i\omega M + \mu + \frac{1}{2}, 2\mu + 1; \frac{1}{\xi}\right) + \xi^{(i\omega/\kappa) - 2i\omega M + \mu + (1/2)} (\xi - 1)^{-(i\omega/2\kappa)} \\
&\quad \times \frac{\Gamma\left(\frac{i\omega}{\kappa} + 1\right) \Gamma(2\mu)}{\Gamma\left(\frac{i\omega}{\kappa} - 2i\omega M + \mu + \frac{1}{2}\right) \Gamma\left(2i\omega M + \mu + \frac{1}{2}\right)} F\left(2i\omega M - \mu + \frac{1}{2}, \frac{i\omega}{\kappa} - 2i\omega M - \mu + \frac{1}{2}, -2\mu + 1; \frac{1}{\xi}\right), \tag{23}
\end{aligned}$$

where the new variable ξ is defined as

$$\xi \equiv \frac{z+1}{2} \quad (24)$$

and μ is

$$\mu \equiv \sqrt{\left(l + \frac{1}{2}\right)^2 + m^2 M^2 - 6\omega^2 M^2}. \quad (25)$$

We have used the linear transformation formulas (15.3.6) of [9] in the second equality of Eq. (22). Using asymptotic expansions (15.7.2) and (15.7.3) of [9] for $|i\omega/\kappa| \gg 1$, we can reduce Eq. (23) to

$$\tilde{\psi}_1(\omega, r_*) \simeq e^{i|\omega/\kappa z|} \left(\frac{2}{z}\right)^{2i|\omega|M} e^{-\pi|\omega|M}, \quad (26)$$

which is valid in the region $1 \ll z \ll 1/\kappa M$, and will be used for asymptotic matching with the solutions given in $z \gg 1$.

B. Solutions for $z \gg 1$

Expanding the wave equation (11) as a power series in $1/z$ and truncating terms of order $1/z$ and higher, we obtain

$$\begin{aligned} \frac{d^2 u}{dx^2} + \frac{2}{x} \frac{du}{dx} + \left[\omega^2 M^2 - m^2 M^2 + \frac{1}{x} (4\omega^2 M^2 - 2m^2 M^2) \right. \\ \left. + \frac{1}{x^2} \{6\omega^2 M^2 - l(l+1) - m^2 M^2\} + \frac{4\omega^2 M^2}{x^3} + \frac{\omega^2 M^2}{x^4} \right. \\ \left. + \frac{2}{x(x+1)^2} \right] u = 0, \end{aligned} \quad (27)$$

introducing the new variable x defined as

$$x \equiv \kappa M z \quad (28)$$

and the function u defined as

$$\tilde{\psi} \equiv (x+1)u. \quad (29)$$

We can give the approximate solutions for Eq. (27) using transcendental functions in the regions $x \ll 1$ and $x \gg 1$, respectively, although it is difficult to find the exact solutions valid in the whole range of x .

1. Solutions for $x \ll 1$

Our strategy to find the approximate solutions for Eq. (27) is to truncate terms of order x^{-1} and higher in the coefficients of u , since these can be smaller than other terms for $x \ll 1$, and to change the variable x to

$$s = \frac{2i\omega M}{x}. \quad (30)$$

Then, Eq. (27) can be approximated by

$$\begin{aligned} \frac{d^2 u}{dx^2} + \frac{2}{x} \frac{du}{dx} + \left[\frac{1}{x^4} \omega^2 M^2 + \frac{1}{x^3} 4\omega^2 M^2 \right. \\ \left. + \frac{1}{x^2} \{6\omega^2 M^2 - l(l+1) - m^2 M^2\} \right] u = 0, \end{aligned} \quad (31)$$

and we can describe the solution of Eq. (31) using the Whittaker's functions

$$u = a_1 W_{\sigma_1, \mu} \left(\frac{2i\omega M}{x} \right) + a_2 W_{-\sigma_1, \mu} \left(-\frac{2i\omega M}{x} \right), \quad (32)$$

where

$$\sigma_1 = -2i\omega M. \quad (33)$$

The asymptotic expansions for $|2i\omega M/x| \gg 1$ lead to

$$W_{\sigma_1, \mu} \left(\frac{2i\omega M}{x} \right) \sim e^{-i(\omega/\kappa z)} \left(i \frac{2\omega}{\kappa z} \right)^{-2i\omega M}, \quad (34)$$

which is necessary for asymptotic matching in the overlap region with the solutions in the region $z \ll 1/\kappa M$. On the other hand, using Eqs. (13.1.3), (13.1.4), and (13.1.33) of [9], we can reduce Eq. (32) to

$$\begin{aligned} W_{\sigma_1, \mu} \left(\frac{2i\omega M}{x} \right) \sim \frac{\Gamma(-2\mu)}{\Gamma\left(\frac{1}{2} - \mu - \sigma_1\right)} \left(\frac{2i\omega M}{x} \right)^{\mu+(1/2)} \\ + \frac{\Gamma(2\mu)}{\Gamma\left(\frac{1}{2} + \mu - \sigma_1\right)} \left(\frac{2i\omega M}{x} \right)^{-\mu+(1/2)}, \end{aligned} \quad (35)$$

if the asymptotic expansions are applied in the region $|2i\omega M/x| \ll 1$ as an analytic extension.

2. Solutions for $x \gg 1$

Contrary to the region $x \ll 1$, truncating terms of order x^{-3} and higher in the coefficients of u in Eq. (27), since these can be smaller than other terms for $x \gg 1$, we can approximate Eq. (27) by

$$\begin{aligned} \frac{d^2 u}{dx^2} + \frac{2}{x} \frac{du}{dx} + \left[\omega^2 M^2 - m^2 M^2 + \frac{1}{x} (4\omega^2 M^2 - 2m^2 M^2) \right. \\ \left. + \frac{1}{x^2} \{6\omega^2 M^2 - l(l+1) - m^2 M^2\} \right] u = 0. \end{aligned} \quad (36)$$

Introducing the function Z defined as

$$u = \frac{Z}{x}, \quad (37)$$

we can reduce Eq. (36) into

$$\frac{d^2 Z}{dx^2} + \left[\omega^2 M^2 - m^2 M^2 + \frac{1}{x} (4\omega^2 M^2 - 2m^2 M^2) + \frac{1}{x^2} \{6\omega^2 M^2 - l(l+1) - m^2 M^2\} \right] Z = 0. \quad (38)$$

Then we can write solutions for Eq. (38) using Whittaker's functions:

$$u = b_1 \frac{M_{\sigma_2, \mu}(2\varpi Mx)}{x} + b_2 \frac{M_{\sigma_2, -\mu}(2\varpi Mx)}{x}, \quad (39)$$

where

$$\sigma_2 = -2\varpi M + \frac{m^2 M}{\varpi}. \quad (40)$$

if estimated in the extended region $|2\varpi Mx| \ll 1$, we obtain

$$M_{\sigma_2, \mu}(2\varpi Mx) \sim (2\varpi Mx)^{\mu+(1/2)}, \quad (41)$$

using Eqs. (13.1.4) and (13.1.32) of [9]. The solution $\tilde{\psi}_2$ satisfying the boundary condition (13) is

$$\tilde{\psi}_2 = W_{\sigma_2, \mu}(2\varpi Mx) \sim e^{-\varpi Mx} (2\varpi Mx)^{\sigma_2} \quad (42)$$

for $|2\varpi Mx| \rightarrow \infty$.

C. Matching

We can match both asymptotic behaviors (26) at $z \ll 1/\kappa M$ and (34) at $x \ll 1$ in the overlap region $1 \ll z \ll 1/(\kappa M)$ in order to determine the coefficients a_1 and a_2 . On the other hand, we find that both asymptotic expressions (35) and (41), which are the results due to analytic extensions from one region into the other, have similar forms. So we can match these smoothly in order to determine the coefficients b_1 and b_2 . In addition, considering the boundary conditions (22) and (42) imposed on $\tilde{\psi}_1$ and $\tilde{\psi}_2$, respectively, we can determine the coefficients α and β in Eq. (14) as follows:

$$\begin{aligned} \alpha(|\omega|, \varpi) &= \beta(e^{i\pi} |\omega|, \varpi) \\ &= \left[\frac{\Gamma(2\mu)\Gamma(2\mu+1)(2\varpi M)^{-\mu+(1/2)} e^{i(\pi/2)[-\mu-(1/2)]}}{\Gamma(\frac{1}{2} + \mu - \sigma_2)(2|\omega|M)^{\mu+(1/2)} \Gamma(\frac{1}{2} + \mu + 2i|\omega|M)} \right. \\ &\quad \left. + \frac{\Gamma(-2\mu)\Gamma(-2\mu+1)(2\varpi M)^{\mu+(1/2)} e^{i(\pi/2)[\mu-(1/2)]}}{\Gamma(\frac{1}{2} - \mu - \sigma_2)(2|\omega|M)^{-\mu+(1/2)} \Gamma(\frac{1}{2} - \mu + 2i|\omega|M)} \right] \left(\frac{|\omega|}{\kappa} \right)^{2i|\omega|M} e^{-\pi|\omega|M} \end{aligned} \quad (43)$$

and

$$\begin{aligned} \beta(|\omega|, \varpi) &= \alpha(e^{i\pi} |\omega|, \varpi) \\ &= \left[\frac{\Gamma(2\mu)\Gamma(2\mu+1)(2\varpi M)^{-\mu+(1/2)} e^{i(\pi/2)[\mu+(1/2)]}}{\Gamma(\frac{1}{2} + \mu - \sigma_2)(2|\omega|M)^{\mu+(1/2)} \Gamma(\frac{1}{2} + \mu - 2i|\omega|M)} \right. \\ &\quad \left. + \frac{\Gamma(-2\mu)\Gamma(-2\mu+1)(2\varpi M)^{\mu+(1/2)} e^{i(\pi/2)[-\mu+(1/2)]}}{\Gamma(\frac{1}{2} - \mu - \sigma_2)(2|\omega|M)^{-\mu+(1/2)} \Gamma(\frac{1}{2} - \mu - 2i|\omega|M)} \right] \left(\frac{|\omega|}{\kappa} \right)^{-2i|\omega|M} e^{-\pi|\omega|M}. \end{aligned} \quad (44)$$

IV. INTERMEDIATE LATE-TIME TAILS

We consider the late-time behaviors of G^C at the time scale

$$mt \gg 1, \quad (45)$$

when the decaying tails will dominate. Hod and Piran [4] pointed out that for the scalar field with small mass, namely $mM \ll 1$, the dominant behavior is given by Eq. (1) at the intermediate late times in the range

$$mM \ll mt \ll \frac{1}{(mM)^2}. \quad (46)$$

In this section we check the validity of Eqs. (43) and (44), by deriving the intermediate-tail behaviors. Following Hod and Piran [4], the effective contribution to the integral in Eq. (17) is claimed to be limited to the range $|\omega - m| = O(1/t)$ or equivalently $\varpi = O(\sqrt{m/t})$. This is due to the rapidly oscillating term $e^{-i\omega t}$ which leads to a mutual cancellation between the positive and the negative parts of the integrand.

Then, in the time scale given by Eq. (46) we note that the frequency range $\varpi = O(\sqrt{m/t})$ leads to the inequality

$$\sigma_2 \ll 1. \quad (47)$$

The factor σ_2 , including the field's parameter m coupled with space-time parameter M , originates from the terms of order x^{-1} in the coefficients of u in Eqs. (27) or (36). If the relation (47) is satisfied, the wave equation at the far region can be approximated by that of flat space time, which means that the effects of backscattering due to space-time curvature has not dominated yet. In other words, the value of σ_2 which gives effective contributions to the integral (17) represents a degree of the domination of the backscattering.

The relation (47) allows us to obtain the approximations of α and β as follows:

$$\begin{aligned} \alpha(|\omega|, \varpi) \sim & \left[\frac{\Gamma(2l+1+2\epsilon_\mu)\Gamma(2l+2+2\epsilon_\mu)}{\Gamma(l+1+\epsilon_\mu-\sigma_2)\Gamma(l+1+\epsilon_\mu+2i|\omega|M)} \right. \\ & \times (2\varpi M)^{-l-\epsilon_\mu} (2|\omega|M)^{-l-1-\epsilon_\mu} \\ & \times e^{i(\pi/2)(-l-1-\epsilon_\mu)} \\ & + \frac{\Gamma(-2l-1-2\epsilon_\mu)\Gamma(-2l-2\epsilon_\mu)}{\Gamma(-l-\epsilon_\mu-\sigma_2)\Gamma(-l-\epsilon_\mu+2i|\omega|M)} \\ & \times (2\varpi M)^{l+1+\epsilon_\mu} (2|\omega|M)^{l+\epsilon_\mu} e^{i(\pi/2)(l+\epsilon_\mu)} \left. \right] \\ & \times \left(\frac{|\omega|}{\kappa} \right)^{2i|\omega|M} e^{-|\omega|M}, \quad (48) \end{aligned}$$

and

$$\begin{aligned} \beta(|\omega|, \varpi) \sim & \left[\frac{\Gamma(2l+1+2\epsilon_\mu)\Gamma(2l+2+2\epsilon_\mu)}{\Gamma(l+1+\epsilon_\mu-\sigma_2)\Gamma(l+1+\epsilon_\mu-2i|\omega|M)} \right. \\ & \times (2\varpi M)^{-l-\epsilon_\mu} (2|\omega|M)^{-l-1-\epsilon_\mu} e^{i(\pi/2)(l+1+\epsilon_\mu)} \\ & + \frac{\Gamma(-2l-1-2\epsilon_\mu)\Gamma(-2l-2\epsilon_\mu)}{\Gamma(-l-\epsilon_\mu-\sigma_2)\Gamma(-l-\epsilon_\mu-2i|\omega|M)} \\ & \times (2\varpi M)^{l+1+\epsilon_\mu} (2|\omega|M)^{l+\epsilon_\mu} e^{i(\pi/2)(-l-\epsilon_\mu)} \left. \right] \\ & \times \left(\frac{|\omega|}{\kappa} \right)^{-2i|\omega|M} e^{-|\omega|M}, \quad (49) \end{aligned}$$

where

$$\epsilon_\mu \equiv \mu - \left(l + \frac{1}{2} \right) \simeq O(mM) \ll 1. \quad (50)$$

Expanding the ratio α/β as a power series in mM , we can approximate it as follows:

$$\begin{aligned} \frac{\alpha(|\omega|, \varpi)}{\beta(|\omega|, \varpi)} &= \frac{\alpha(|\omega|, e^{-i\pi}\varpi)}{\beta(|\omega|, e^{-i\pi}\varpi)} \\ &\sim \frac{l!^4}{(2l)!^2(2l+1)!^2} (2M)^{4l+2} |\omega|^{2l+1} \varpi^{2l+1} 2i. \quad (51) \end{aligned}$$

Substituting Eq. (51) into Eq. (17), we obtain

$$\begin{aligned} G^C(r_*, r'_*; t) &= \frac{l!^4}{(2l)!^2(2l+1)!^2} (2M)^{4l+2} \\ &\times \int_0^m \omega^{2l+1} \varpi^{2l+1} \tilde{\psi}_1(r_*, \omega) \tilde{\psi}_1(r'_*, \omega) \\ &\times e^{-i\omega t} d\omega + (\text{complex conjugate}), \quad (52) \end{aligned}$$

which is similar to Eq. (29) in [4], giving the damping exponent in Eq. (1).

Different from [4], our analytical calculation is not based on the flat-space approximation. The intermediate tails dominate in the range (46), when the integrand can be approximated using the relation (47). It is easy to find that the larger the field's mass is, the sooner it leaves the intermediate tails, and the phase does not appear in the case of $mM \gtrsim 1$.

V. ASYMPTOTIC LATE-TIME TAILS

It is obvious from our calculation that the intermediate tail is not a final pattern of decay but should be replaced by another one, because the dominant contribution to the integral (17) is out of the region (47) after the intermediate late times (46). The change into another phase was also numerically suggested in [4]. Physically the change of the tail behavior will be a result of dominant backscattering due to space-time curvature, which is the effect beyond the flat-space approximation. What kind of wave pattern dominates at very late times? In addition, we must reveal late-time tails in the $mM \gtrsim 1$ case of large field mass, for which the intermediate tails do not appear. In this section we study a tail behavior dominant at asymptotic late times

$$mt \gg \frac{1}{m^2 M^2}, \quad (53)$$

when the effective contribution to the integral (17) arises from the region

$$\sigma_2 \simeq \frac{m^2 M}{\varpi} \gg 1, \quad (54)$$

different from the inequality (47) at intermediate late times. The coefficients $\alpha(\omega, \varpi)$ and $\beta(\omega, \varpi)$ are approximated for the inequality (54) by

$$\begin{aligned}
\alpha(|\omega|, \varpi) &= \beta(e^{i\pi}|\omega|, \varpi) \\
&\simeq \frac{1}{\sqrt{2\pi}} e^{(m^2 M/\varpi)} (2m^2 M^2)^{-(m^2 M/\varpi)+2\varpi M} (2\varpi M)^{-2\varpi M+(m^2 M/\varpi)+(1/2)} \\
&\quad \times \left[\frac{\Gamma(2\mu)\Gamma(2\mu+1)(2m^2 M^2)^{-\mu}(2|\omega|M)^{-\mu-(1/2)} e^{i(\pi/2)[- \mu-(1/2)]} }{\Gamma(\frac{1}{2} + \mu + 2i|\omega|M)} \right. \\
&\quad \left. + \frac{\Gamma(-2\mu)\Gamma(-2\mu+1)(2m^2 M^2)^\mu(2|\omega|M)^{\mu-(1/2)} e^{i(\pi/2)[\mu-(1/2)]} }{\Gamma(\frac{1}{2} - \mu + 2i|\omega|M)} \right] \left(\frac{|\omega|}{\kappa} \right)^{2i|\omega|M} e^{-\pi|\omega|M} \quad (55)
\end{aligned}$$

and

$$\begin{aligned}
\beta(|\omega|, \varpi) &= \alpha(e^{i\pi}|\omega|, \varpi) \\
&\simeq \frac{1}{\sqrt{2\pi}} e^{(m^2 M/\varpi)} (2m^2 M^2)^{-(m^2 M/\varpi)+2\varpi M} (2\varpi M)^{-2\varpi M+(m^2 M/\varpi)+(1/2)} \\
&\quad \times \left[\frac{\Gamma(2\mu)\Gamma(2\mu+1)(2m^2 M^2)^{-\mu}(2|\omega|M)^{-\mu-(1/2)} e^{i(\pi/2)[\mu+(1/2)]} }{\Gamma(\frac{1}{2} + \mu - 2i|\omega|M)} \right. \\
&\quad \left. + \frac{\Gamma(-2\mu)\Gamma(-2\mu+1)(2m^2 M^2)^\mu(2|\omega|M)^{\mu-(1/2)} e^{i(\pi/2)[- \mu+(1/2)]} }{\Gamma(\frac{1}{2} - \mu - 2i|\omega|M)} \right] \left(\frac{|\omega|}{\kappa} \right)^{-2i|\omega|M} e^{-\pi|\omega|M}. \quad (56)
\end{aligned}$$

Thus the contribution from this part corresponding to the dotted lines in Fig. 1 to the Green's function given by

$$\frac{1}{4\pi i} \int_{\text{dotted lines}} \frac{1}{\omega} \frac{\alpha(\omega, \varpi)}{\beta(\omega, \varpi)} \tilde{\psi}_1(r_*, \omega) \tilde{\psi}_1(r'_*, \omega) e^{-i\omega t} d\omega \quad (57)$$

is $O(t^{-1})$ at most, because $\alpha(\omega, e^{\pm i\pi}\varpi)$ and $\beta(\omega, e^{\pm i\pi}\varpi)$ converge in the limit $|\omega| \rightarrow m$. On the other hand, $\alpha(\omega, \varpi)$ and $\beta(\omega, \varpi)$ are reduced to

$$\frac{\alpha(|\omega|, \varpi)}{\beta(|\omega|, \varpi)} = \frac{\beta(e^{i\pi}|\omega|, \varpi)}{\alpha(e^{i\pi}|\omega|, \varpi)} \simeq \frac{\gamma^* e^{-i\pi\sigma_2} + \eta^* e^{i\pi\sigma_2}}{\gamma e^{i\pi\sigma_2} + \eta e^{-i\pi\sigma_2}}, \quad (58)$$

for the limit Eq. (54), where

$$\begin{aligned}
\gamma &= \frac{\Gamma(-2\mu)\Gamma(-2\mu+1)(2m^2 M^2)^\mu(2|\omega|M)^{\mu-(1/2)}}{\Gamma(\frac{1}{2} - \mu - 2i|\omega|M)} \\
&\quad \times e^{i(\pi/2)[\mu+(1/2)]} \\
&\quad + \frac{\Gamma(2\mu)\Gamma(2\mu+1)(2m^2 M^2)^{-\mu}(2|\omega|M)^{-\mu-(1/2)}}{\Gamma(\frac{1}{2} + \mu - 2i|\omega|M)} \\
&\quad \times e^{i(\pi/2)[- \mu+(1/2)]}, \quad (59)
\end{aligned}$$

and

$$\begin{aligned}
\eta &= \frac{\Gamma(-2\mu)\Gamma(-2\mu+1)(2m^2 M^2)^\mu(2|\omega|M)^{\mu-(1/2)}}{\Gamma(\frac{1}{2} - \mu - 2i|\omega|M)} \\
&\quad \times e^{i(\pi/2)[-3\mu+(1/2)]} \\
&\quad + \frac{\Gamma(2\mu)\Gamma(2\mu+1)(2m^2 M^2)^{-\mu}(2|\omega|M)^{-\mu-(1/2)}}{\Gamma(\frac{1}{2} + \mu - 2i|\omega|M)} \\
&\quad \times e^{i(\pi/2)[3\mu+(1/2)]}. \quad (60)
\end{aligned}$$

Therefore we find the contribution from this part corresponding to the dashed line in Fig. 1 to the Green's function to be approximated by

$$\begin{aligned}
&\frac{1}{4\pi i} \int_0^m \frac{1}{\omega} \frac{\alpha(\omega, \varpi)}{\beta(\omega, \varpi)} e^{-i\omega t} \tilde{\psi}_1(r_*, \omega) \tilde{\psi}_1(r'_*, \omega) d\omega \\
&\quad + (\text{complex conjugate}) \\
&\simeq \frac{1}{4\pi m i} \tilde{\psi}_1(r_*, m) \tilde{\psi}_1(r'_*, m) \int_0^m e^{i(2\pi\sigma_2 - \omega t)} e^{i\varphi} d\omega \\
&\quad + (\text{complex conjugate}), \quad (61)
\end{aligned}$$

where the phase φ is defined by

$$e^{i\varphi} = \frac{\eta^* + \gamma^* e^{-2i\pi\sigma_2}}{\eta + \gamma e^{2i\pi\sigma_2}} \quad (62)$$

and it remains in the range $0 \leq \varphi \leq 2\pi$, even if σ_2 becomes very large, since we have

$$|\eta|^2 - |\gamma|^2 = \frac{\pi}{|\omega|M} e^{2\pi|\omega|M} > 0. \quad (63)$$

At very late times when Eqs. (45) and (54) are satisfied, both terms of $e^{i\omega t}$ and $e^{2i\pi\sigma_2}$ are rapidly oscillating. In a physical meaning, scalar waves are mixed states with multiple phases backscattered by space-time curvature, and most of these waves cancel each other out by those of the inverse phase. If the value of $2\pi\sigma_2 - \omega t$ in Eq. (61) is stationary at $\omega = \omega_0$, i.e.,

$$\frac{d}{d\omega}(2\pi\sigma_2 - \omega t) = 0, \quad (64)$$

particular waves with the frequency ω_0 remain without cancellation, and contribute dominantly to the tail behaviors. In such a case we can evaluate the integral (61) as the effective contribution from the immediate vicinity of the saddle point ω_0 . This method, which is called the saddle-point integration, allows us to evaluate accurately the asymptotic behaviors of Bessel functions as a well-known example. We can find a solution for Eq. (64),

$$\varpi_0 \equiv \sqrt{m^2 - \omega_0^2} \approx \left(\frac{2\pi m^3 M}{t} \right)^{1/3}, \quad (65)$$

in the limit $\omega_0 \approx m$. In order for the saddle point (65) to exist in the region (54), where $e^{2i\pi\sigma_2}$ are rapidly oscillating as a function of ω , we need the additional relation

$$mt \gg mM. \quad (66)$$

Approximating the integration (61) by the contribution from the immediate vicinity of ω_0 , we obtain

$$\begin{aligned} & \frac{1}{4\pi i m} \int e^{i(d^2/d\omega^2)(2\pi\sigma_2 - \omega t)|_{\omega=\omega_0}} (\omega - \omega_0)^2 e^{i\varphi(\omega_0)} d\omega \\ & \sim \frac{i}{4\sqrt{3}} (2\pi)^{5/6} (mM)^{1/3} (mt)^{-5/6} e^{imt} e^{i\varphi(\omega_0)}, \end{aligned} \quad (67)$$

through the formula

$$\int_{-\infty}^{\infty} \cos(x^2) dx = \int_{-\infty}^{\infty} \sin(x^2) dx = \sqrt{\frac{\pi}{2}}. \quad (68)$$

Taking the decay rate into account, we can neglect the contribution from Eq. (57) to G^C in comparison with that from Eq. (67). Therefore tails such as Eq. (67) dominate at asymptotic late times. Finally we arrive at the asymptotic late-time tail as

$$\begin{aligned} G^C(r_*, r'_*; t) & \approx \frac{1}{2\sqrt{3}} (2\pi)^{5/6} (mM)^{1/3} (mt)^{-5/6} \\ & \times \sin(mt) \tilde{\psi}_1(r_*, m) \tilde{\psi}_1(r'_*, m), \end{aligned} \quad (69)$$

of which the decay rate is independent of the location r_* .

It is found that the time, when the conditions for the application of the saddle-point integration, namely, Eqs. (45), (53), and (66) are all satisfied, must come sooner or later independent of field mass, and the tail (69) is the asymptotic behavior at late times in the limit $mt \rightarrow \infty$.

VI. SUMMARY AND DISCUSSIONS

In this paper we have investigated mass-induced behaviors which appear in late-time tails of classical massive scalar fields in nearly extreme Reissner-Nordström background. If the field mass is small, namely $mM \ll 1$, the intermediate tails given by Eq. (1) have been shown to dominate at the intermediate late-time $mM \ll mt \ll 1/(mM)^2$, consistently with [4] (see also [5]). Our main result is the asymptotic tail with the decay rate of $t^{-5/6}$, which is interestingly independent of the field mass m and the angular momentum parameter l . This behaviors of inverse power-law decay supports the numerical results in [5,10].

Late-time tail behaviors are generally caused by the domination of the backscattering from far regions. It is found the asymptotic tail of massive scalar fields (69) appears when the effective contribution to the integral (17) arises from the region (54), namely, when the backscattering due to space-time curvature dominates. Further, the frequencies of waves which contribute to the backscattering are sharply peaked about ω_0 . These facts suggest that the asymptotic $t^{-5/6}$ tail is caused by a *resonance* backscattering due to spacetime curvature.

We can also clarify the resonant picture from a viewpoint of the time scale when the $t^{-5/6}$ tail dominates. The basic condition for the tail dominance is given by Eq. (45). However, for $mM \ll 1$, the $t^{-5/6}$ tail requires the additional condition (54), which gives $mt \gg 1/m^2 M^2$. On the other hand, for large field mass $mM \gg 1$, the larger mM is, the later the $t^{-5/6}$ tail begins to dominate, because the tail requires the further condition $\varpi_0/m \ll 1$ for Eq. (65) in addition to the conditions (45) and (54), which gives $mt \gg mM$. Therefore the time scale when the $t^{-5/6}$ tail dominates will become minimum at $mM \approx O(1)$, which means that the most effective backscattering occurs for such massive scalar fields at late times. Here we note that the time scale when the $t^{-5/6}$ tail dominates is determined by the black-hole radius M . It is conjectured that the slow decay of $t^{-5/6}$ originates from the existence of resonant enhancement of massive scalar waves with the peculiar frequency ω_0 near the horizon. In conclusion, we claim that resonance behaviors in field-mass dependence are not peculiar to quantum scalar fields but manifest also in classical scalar fields.

In this paper we have calculated the tail behaviors in nearly extremal limit, because we are motivated by the previous work [2]. The extension of our calculation into nonextremal case remains in future works, to investigate whether our result in this paper is a special feature of the extremal case or not.

ACKNOWLEDGMENTS

The authors thank A. Hosoya, M. Sakagami, A. Ohashi, and the colleagues of the CG laboratory at Nagoya University for valuable discussions and comments. H.K. thanks T. Konishi and Y. Hirata for useful advice on the analysis of differential equations.

- [1] L. Randall and R. Sundrum, Phys. Rev. Lett. **83**, 4690 (1999).
- [2] A. Tomimatsu and H. Koyama, Phys. Rev. D **61**, 124010 (2000).
- [3] A. A. Starobinskii and I. D. Novikov (unpublished).
- [4] S. Hod and T. Piran, Phys. Rev. D **58**, 044018 (1998).
- [5] L. M. Burko, in 15th International Conference on General Relativity and Gravitation, Pune, 1997, p. 143.
- [6] R.H. Price, Phys. Rev. D **5**, 2419 (1972).
- [7] E. W. Leaver, Phys. Rev. D **34**, 384 (1986).
- [8] A. Ori, Gen. Relativ. Gravit. **29**, 881 (1997); L. Barack and A. Ori, Phys. Rev. Lett. **82**, 4388 (1999); Phys. Rev. D **60**, 124005 (1999).
- [9] *Handbook of Mathematical Functions*, edited by M. Abramowitz and I.A. Stegun (Dover, New York, 1970).
- [10] L. M. Burko and A. Ori, Phys. Rev. D **56**, 7820 (1997).